JCI insight

RESEARCH ARTICLE

Erythromycin inhibits neutrophilic inflammation and mucosal disease by upregulating DEL-1

Tomoki Maekawa,[1,2,3] Hikaru Tamura,[1,2,3] Hisanori Domon,[1,2] Takumi Hiyoshi,[1,2] Toshihito Isono,[2] Daisuke Yonezawa,[1,4] Naoki Hayashi,[5] Naoki Takahashi,[3] Koichi Tabeta,[3] Takeyasu Maeda,[1,6] Masataka Oda,[5] Athanasios Ziogas,[7] Vasileia Ismini Alexaki,[7] Triantafyllos Chavakis,[7,8] Yutaka Terao,[1,2] and George Hajishengallis[9]

[1]Center for Advanced Oral Science, [2]Division of Microbiology and Infectious Diseases, [3]Division of Periodontology, and [4]Division of Oral Science for Health Promotion, Graduate School of Medical and Dental Sciences, Niigata University, Niigata, Japan. [5]Department of Microbiology and Infection Control Sciences, Kyoto Pharmaceutical University, Yamashina, Japan. [6]Faculty of Dental Medicine, Universitas Airlangga, Surabaya, Indonesia. [7]Institute of Clinical Chemistry and Laboratory Medicine, Faculty of Medicine and University Clinic Carl Gustav Carus, TU Dresden, Dresden, Germany. [8]Centre for Cardiovascular Science, Queen's Medical Research Institute, College of Medicine and Veterinary Medicine, University of Edinburgh, Edinburgh, United Kingdom. [9]Laboratory of Innate Immunity and Inflammation, Department of Basic and Translational Sciences, Penn Dental Medicine, University of Pennsylvania, Philadelphia, Pennsylvania, USA.

Macrolide antibiotics exert antiinflammatory effects; however, little is known regarding their immunomodulatory mechanisms. In this study, using 2 distinct mouse models of mucosal inflammatory disease (LPS-induced acute lung injury and ligature-induced periodontitis), we demonstrated that the antiinflammatory action of erythromycin (ERM) is mediated through upregulation of the secreted homeostatic protein developmental endothelial locus-1 (DEL-1). Consistent with the anti–neutrophil recruitment action of endothelial cell–derived DEL-1, ERM inhibited neutrophil infiltration in the lungs and the periodontium in a DEL-1–dependent manner. Whereas ERM (but not other antibiotics, such as josamycin and penicillin) protected against lethal pulmonary inflammation and inflammatory periodontal bone loss, these protective effects of ERM were abolished in *Del1*-deficient mice. By interacting with the growth hormone secretagogue receptor and activating JAK2 in human lung microvascular endothelial cells, ERM induced DEL-1 transcription that was mediated by MAPK p38 and was CCAAT/enhancer binding protein–β dependent. Moreover, ERM reversed IL-17–induced inhibition of DEL-1 transcription, in a manner that was dependent not only on JAK2 but also on PI3K/AKT signaling. Because DEL-1 levels are severely reduced in inflammatory conditions and with aging, the ability of ERM to upregulate DEL-1 may lead to a novel approach for the treatment of inflammatory and aging-related diseases.

Authorship note: TM, YT, and GH contributed equally as co–senior authors.

Conflict of interest: The authors have declared that no conflict of interest exists.

Submitted: January 24, 2020
Accepted: June 24, 2020
Published: June 30, 2020.

Reference information: *JCI Insight*. 2020;5(15):e136706. https://doi.org/10.1172/jci.insight.136706.

Introduction

Macrolides have well-established antimicrobial and antivirulence effects that can be used to treat infectious diseases (1, 2). For instance, we previously demonstrated that, in the context of macrolide-resistant *Streptococcus pneumoniae* (*S. pneumoniae*) infection, subminimum inhibitory concentrations of macrolides inhibit the release of pneumococcal autolysin, thereby preventing cell lysis and pneumolysin release (3). However, macrolides are also applied to treat noninfectious diseases, such as cystic fibrosis (4), chronic obstructive pulmonary disease (COPD) (5, 6), acute respiratory distress syndrome (7), and certain forms of asthma (8). Intriguingly, according to systematic reviews, macrolides exert a broad range of immunomodulatory actions in a manner distinct from their bactericidal activity (9). Thus, macrolides may affect not only bacteria but also components of the human immune system. Although the concept of using macrolides for immune modulation was reported 40 years ago (10), the exact mechanism(s) underlying the immunomodulatory effects of macrolides remains uncertain. The frequent usage of macrolides as antibiotics (which requires higher dose concentrations than when used for immunomodulation, ref. 11) is problematic due to the potential development of drug-resistant bacteria. Indeed, we have recently reported that 82% of *S. pneumoniae*

isolates were nonsusceptible to azithromycin, a 14-membered macrolide (12). Therefore, it is important to identify and mechanistically understand the immunomodulatory effects of macrolides, distinct from their antimicrobial action, and exploit them therapeutically in the context of inflammatory disorders.

The immunomodulatory effects of macrolides include the regulation of inflammation, whereby the most frequent and consistent observation is inhibition of neutrophilic inflammation (1, 9), an activity shared with the integrin-binding secreted protein developmental endothelial locus-1 (DEL-1). DEL-1 has emerged as an important factor in neutrophil homeostasis in the context of both the initiation and the resolution of inflammation (13–15). Specifically, DEL-1 modulates the production and recruitment of neutrophils and also the clearance of apoptotic neutrophils by tissue macrophages, which are thereby reprogrammed to acquire a proresolving phenotype (14–16). DEL-1 deficiency in mice is associated with increased pulmonary inflammation as well as susceptibility to periodontitis and experimental autoimmune encephalomyelitis (model for multiple sclerosis), accompanied by excessive neutrophil infiltration and IL-17–driven tissue destruction (13, 15, 17, 18). Moreover, humans with acute respiratory distress syndrome display increased circulating and alveolar levels of IL-17 (19). Intriguingly, the expression levels of DEL-1 and IL-17 are inversely correlated in inflammatory disorders (such as periodontitis, airway inflammation, and multiple sclerosis), and IL-17 inhibits endothelial cell expression of DEL-1 (13, 17, 18, 20, 21).

In the present study, therefore, we investigated whether and how the antiinflammatory effects of macrolides are dependent on DEL-1 as well as the underlying mechanisms. We demonstrated that erythromycin (ERM), a 14-membered macrolide, ameliorates neutrophilic inflammation in the lungs and the periodontal tissue and protects against lethal pulmonary inflammation and periodontal bone loss, respectively, by upregulating DEL-1 expression and reversing the inhibitory effect of IL-17 on DEL-1 expression. We also dissected the underlying signaling pathways. By interacting with the growth hormone secretagogue receptor (GHSR), ERM activates JAK2 signaling, which leads to DEL-1 transcription that is MAPK p38 mediated and CCAAT/enhancer binding protein–β (C/EBPβ) dependent, as well as to PI3K/AKT-mediated reversal of the glycogen synthase kinase 3β–dependent (GSK3β-dependent) inhibitory effect of IL-17 on DEL-1 expression. Given that DEL-1 expression is diminished in inflammatory conditions and with advanced age (13), the ability of ERM to upregulate DEL-1 paves the way to new approaches for treating inflammatory and aging-related disorders.

Results

ERM upregulates DEL-1 mRNA and protein levels in vitro and in vivo. To determine whether ERM can regulate neutrophil infiltration by regulating DEL-1 production (13), we first tested whether ERM could induce DEL-1 mRNA and protein in human lung microvascular endothelial cells (HMVECs). As comparative controls, we used the macrolide antibiotics josamycin (JSM) and penicillin (PC). Whereas the 14-membered ring macrolide ERM upregulated *DEL1* mRNA expression, JSM, a 16-membered macrolide, and PC, a β-lactam antibiotic, failed to do so (Figure 1A). In Figure 1 and throughout the in vitro experiments, ERM, JSM, and PC were used at 10 μg/mL, which was the minimum concentration of ERM yielding maximum induction of DEL-1 expression (Supplemental Figure 1; supplemental material available online with this article; https://doi.org/10.1172/jci.insight.136706DS1). The DEL-1 protein levels in HMVEC culture supernatants were measured by ELISA. Consistent with the mRNA data, ERM, but not JSM or PC, induced the production of DEL-1 protein (Figure 1B). Additionally, we evaluated whether administration of ERM induced *Del1* mRNA expression in the lung tissue. To this end, mice were administered with ERM, JSM, or PC daily for 1 week. The mRNA levels of *Del1* in the lung were upregulated only in the ERM-treated group (Figure 1C). These findings suggest that ERM, but not JSM or PC, has the ability to induce DEL-1 expression both in vitro and in vivo.

ERM suppresses neutrophil infiltration and inflammation in the lungs. DEL-1 binds to the lymphocyte function-associated antigen-1 integrin on neutrophils and suppresses their adhesion to intercellular adhesion molecule 1 on vascular endothelial cells, thereby restraining neutrophil recruitment to the lungs (15). Given that ERM can induce DEL-1 expression in the lungs, we next examined whether ERM could suppress neutrophil infiltration in the bronchoalveolar lavage fluid (BALF). To this end, mice were administered with ERM, JSM, PC, or vehicle control (ethanol) intraperitoneally 3 hours before and 24 hours after intratracheal challenge with a sublethal dose (2.5 mg/kg body weight) of LPS (Figure 2A). The mice were euthanized 48 hours after LPS challenge for analysis. The number of neutrophils in the BALF was significantly decreased in the ERM treatment group, whereas there were no differences in neutrophil numbers in the JSM- and

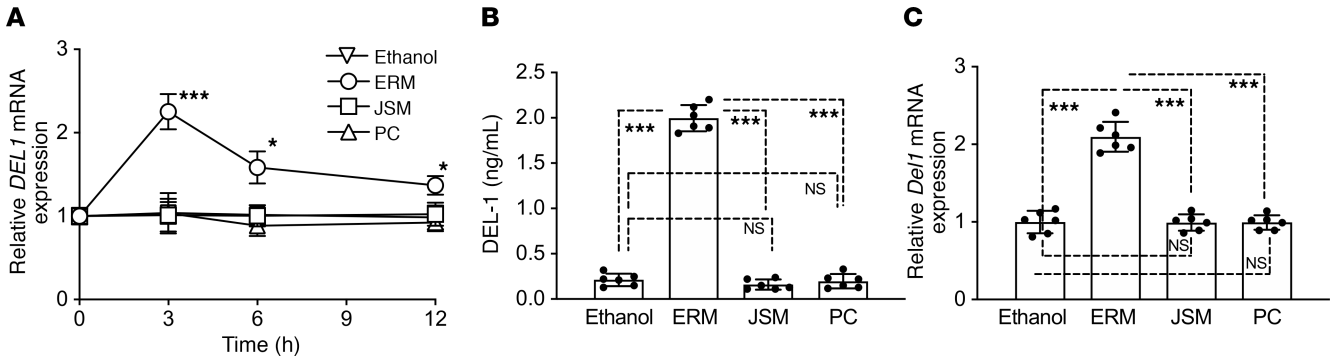

Figure 1. ERM upregulates DEL-1 mRNA and protein levels. (**A**) *DEL1* mRNA transcription was analyzed by quantitative PCR (qPCR) in HMVECs incubated for the indicated time periods with or without ERM (10 μg/mL), JSM (10 μg/mL), or PC (10 μg/mL). Data were normalized against *GAPDH* mRNA and expressed as fold induction relative to treatment with ethanol (vehicle control), which was assigned an average value of 1. (**B**) DEL-1 protein levels in the cell culture supernatants after 6-hour incubation were measured by ELISA. (**C**) *Del1* mRNA transcription in the lung tissue was analyzed by qPCR 24 hours after i.p. injection of ethanol (vehicle control), ERM (20 mg/kg), JSM (20 mg/kg), or PC (20 mg/kg). Data were normalized against *Gapdh* mRNA and expressed as fold induction relative to treatment with ethanol (vehicle control), which was assigned an average value of 1. Data are presented as the mean ± SD; (**A** and **B**: n = 6 sets of HMVECs cultures; and **C**: n = 6 mice/group); (**A**) 2-way ANOVA followed by Holm-Šidák multiple comparisons test; (**B** and **C**) 1-way ANOVA followed by Tukey's multiple comparisons test; *$P < 0.01$, ***$P < 0.0001$ between indicated groups.

PC-treated mice as compared with ethanol-treated control mice (Figure 2B). Consistent with these data, the activity of myeloperoxidase (MPO) in the BALF was significantly decreased by ERM but not by JSM or PC (Figure 2C). Next, we analyzed mRNA expression levels of proinflammatory and antiinflammatory cytokines in harvested mouse lung tissue. ERM treatment suppressed *Il6*, *Il17*, and *Tnf* mRNA expression and upregulated *Del1* and *Il10* mRNA expression, whereas JSM and PC had no significant effects in this regard (Figure 2D). Mean linear intercept (representing mean free distance in airspaces) was increased in the lung compartments in the group of mice administered LPS and ethanol control, but this effect was reversed in mice administered LPS and ERM (Figure 2E). In contrast, the LPS-induced increase of mean linear intercept was not affected by JSM or PC (Figure 2E). H&E staining of lung tissue showed that LPS administration resulted in an increase in airspace size and rupture of alveolar septa, but this effect was prevented by ERM (albeit not by JSM or PC) (Figure 2F). Immunohistochemistry analysis was performed in DEL-1– and neutrophil elastase–stained sections to evaluate the antiinflammatory effect of ERM at 48 hours. DEL-1–expressing cells were observed in the ethanol control–treated group, but DEL-1 staining was essentially absent in the LPS-treated group (Figure 2G), consistent with the reported strong inhibition of DEL-1 expression under inflammatory conditions in the lung (15). Immunofluorescence analysis of sections from the group treated with both LPS and ERM revealed ample staining for DEL-1, suggesting that the paucity of DEL-1 expression due to LPS treatment was reversed by ERM, although not by the other antibiotics tested (Figure 2G). The intensity of DEL-1 staining in the lungs appeared to be inversely associated with elastase staining (marker of neutrophil infiltration); indeed, elastase was readily stained in sections from the group treated with LPS and ethanol, but elastase staining was reduced in the group treated with LPS and ERM (Figure 2G). To examine whether the antiinflammatory effects of ERM in the lungs required the presence of DEL-1, we used *Del1*$^{-/-}$ mice generated by Setsuro Tech through gene editing by electroporation of Cas9 protein (GEEP) methods (22, 23). In contrast to WT mice, in which ERM treatment resulted in reduced staining for neutrophil elastase (Figure 2G), *Del1*$^{-/-}$ mice displayed similar elastase staining in the lungs regardless of whether they were treated with ERM or ethanol control (Figure 2H). As expected, *Del1*$^{-/-}$ mice did not show any staining for DEL-1 (Figure 2H), thus supporting the specificity of DEL-1 staining in WT mice (Figure 2G). These data indicate that ERM induces DEL-1 expression in the lungs and, consistent with the anti–neutrophil recruitment activity of DEL-1 (15), inhibits neutrophil-associated pulmonary inflammation. These data also suggested that ERM may depend on DEL-1 for its antiinflammatory effect, a possibility that was rigorously addressed using a lethal challenge model.

ERM improves mouse survival after LPS-induced acute lung injury in a DEL-1–dependent manner. To further characterize the biological relevance of the ERM-induced upregulation of DEL-1 expression in vivo, we engaged an LPS acute lung injury model in mice using a lethal dose (25 mg LPS/kg body weight) (Figure 3A) (24). In this model, lung injury caused by bacterial LPS administration exhibits microvascular injury and diffuse alveolar damage with pulmonary hemorrhage edema and fibrin deposition (25, 26).

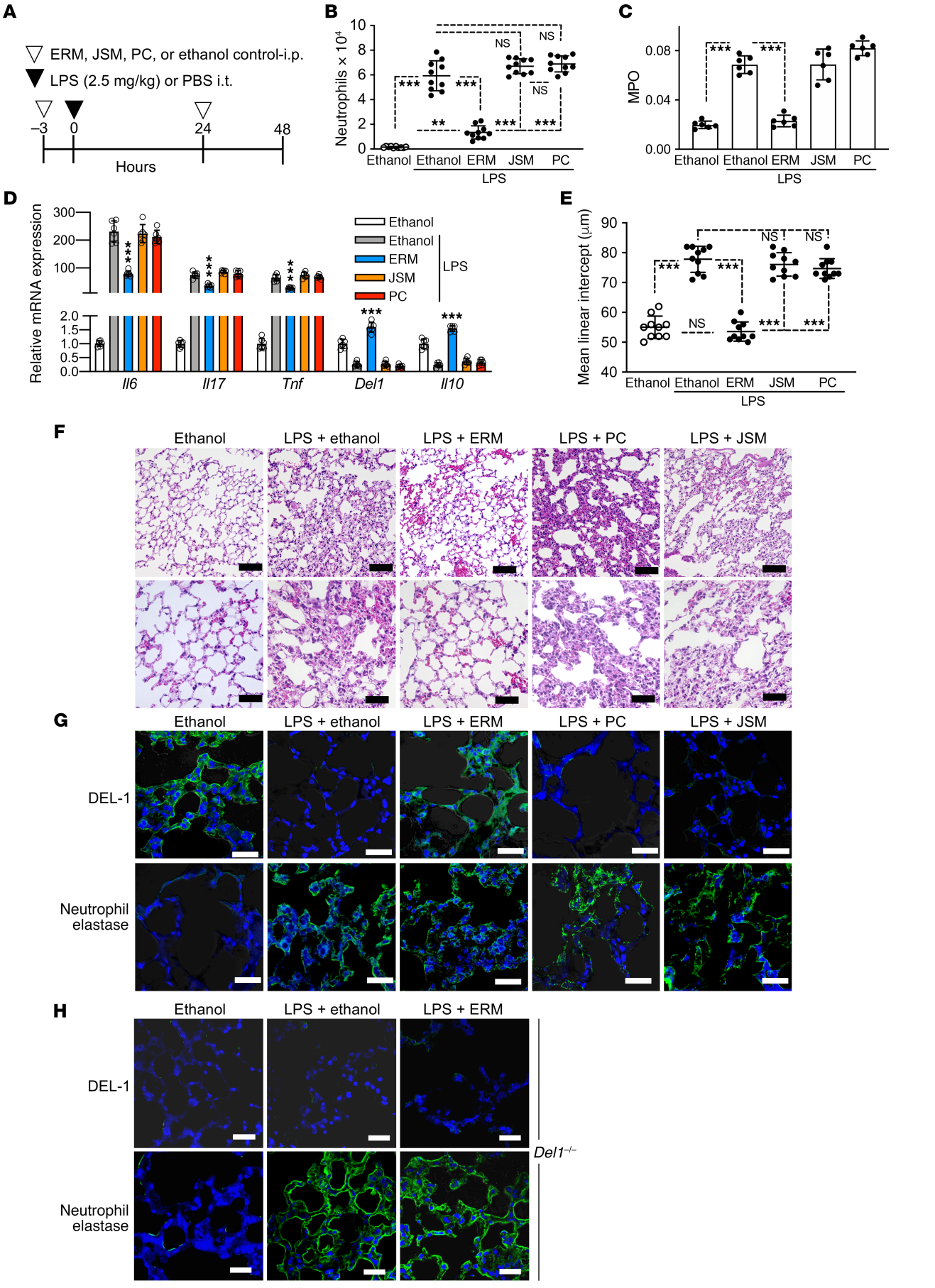
A
ERM, JSM, PC, or ethanol control-i.p.
LPS (2.5 mg/kg) or PBS i.t.
–3
0
24
48
Hours
B
Neutrophils × 10⁴
Ethanol
Ethanol
ERM
JSM
PC
LPS
NS
***
**
C
MPO
0.08
0.04
0.00
D
Relative mRNA expression
Ethanol
Ethanol
ERM
JSM
PC
LPS
Il6
Il17
Tnf
Del1
Il10
E
Mean linear intercept (μm)
F
Ethanol
LPS + ethanol
LPS + ERM
LPS + PC
LPS + JSM
G
DEL-1
Neutrophil elastase
H
Del1−/−

Figure 2. ERM suppresses neutrophil infiltration in BALF. (**A**) Experimental design. *E. coli* LPS (2.5 mg/kg) was administrated intratracheally. ERM (20 mg/kg) or JSM (20 mg/kg), PC (20 mg/kg), or ethanol control (n = 10 mice/group) was administrated i.p. 3 hours before and 24 hours after LPS administration. Samples were collected 48 hours after LPS administration. (**B** and **C**) Neutrophil counts (**B**) and myeloperoxidase (MPO) activity (**C**) in the BALF 48 hours after LPS challenge (**B**: n = 10 mice/group; **C**: n = 6 mice/group). (**D**) The mRNA levels of proinflammatory cytokines (*Il6*, *Il17*, and *Tnf*), *Del1*, and *Il10* in the lung tissue were determined by qPCR 48 hours after LPS challenge (n = 6 mice/group). Data were normalized against *Gapdh* mRNA and expressed as fold induction relative to treatment with ethanol control, which was assigned an average value of 1. (**E**) Mean linear intercept measured in central and peripheral areas of the lungs 48 hours after LPS challenge (n = 10 mice/group). (**F**) Representative images of H&E-stained pulmonary parenchyma 48 hours after LPS challenge. Upper panel: scale bars, 50 μm; lower panel: scale bars, 25 μm. (**G**) IHC of lung tissue in WT mice stained with DEL-1 and neutrophil elastase 48 hours after LPS challenge. Scale bars: 50 μm. (**H**) IHC of lung tissue in *Del1*$^{-/-}$ mice stained with DEL-1 and neutrophil elastase 48 hours after sublethal LPS (2.5 mg/kg) challenge as outlined in panel **A**. Scale bars: 100 μm. Data are presented as the mean ± SD. $^{**}P < 0.01$, $^{***}P < 0.001$ by 1-way ANOVA followed by Tukey's multiple comparisons test.

Treatment with ERM, but not with JSM or PC, significantly reduced mortality in mice subjected to LPS-induced acute lung injury (Figure 3B). Moreover, ERM, but not JSM or PC, caused a significant reduction in IL-17 and TNF serum levels (Figure 3 C and D, respectively) and a significant increase in the serum levels of the antiinflammatory IL-10 (Figure 3E), as compared with ethanol control. In side-by-side experiments, DEL-1–Fc and ERM caused comparable improvement in the survival of mice subjected to LPS-induced acute lung injury (Figure 3F). Similar to ERM, DEL-1–Fc (but not Fc control) reduced the levels of proinflammatory IL-17 and TNF and increased the levels of antiinflammatory IL-10 in the serum (Figure 3, C–E). The improved mouse survival in the ERM– or the DEL-1–Fc –treated mice was accompanied by a significant increase in the oxygen saturation (SpO_2) levels, as compared with treatments with JSM, PC, or ethanol control (Figure 3G). Notably, ERM treatment failed to inhibit neutrophil recruitment to the lungs (Figure 3H) or to improve the survival of *Del1*$^{-/-}$ mice in the LPS-induced lung injury model (Figure 3I). Consistent with the survival results, the serum levels of TNF (Figure 3J) and IL-17 (Figure 3K) were decreased in ERM-treated WT mice but not in ERM-treated *Del1*$^{-/-}$ mice, as compared with their respective ethanol-treated controls. Conversely, the serum levels of IL-10 were increased in ERM-treated WT mice but not in ERM-treated *Del1*$^{-/-}$ mice (Figure 3L). In contrast to ERM, DEL-1–Fc protein administration improved the survival of *Del1*$^{-/-}$ mice subjected to LPS-induced lung injury (Figure 3M). Taken together, these data suggest that DEL-1 is a required effector of the protective effect of ERM treatment of mice exposed to LPS-induced lung injury. In other words, ERM exerts protective effects in vivo through DEL-1–dependent antiinflammatory properties.

ERM suppresses periodontal inflammation and bone loss in a DEL-1–dependent manner. To examine whether the DEL-1–dependent effects of ERM represent a more general principle in protection against inflammatory disorders, we additionally investigated the biological effects of ERM in mice subjected to ligature-induced periodontitis (LIP). The LIP model is well established and mimics human periodontitis, an oral inflammatory disease that affects the integrity of the tissues that surround and support the dentition (e.g., gingiva and alveolar bone) (27); indeed, LIP generates a subgingival biofilm-retentive milieu, leading to Th17- and IL-17–driven inflammation and bone loss, features that are shared by human periodontitis (14, 28). Periodontal bone loss was induced for 9 days by ligating the maxillary second molar and leaving the contralateral tooth unligated (baseline control) (Figure 4A). Systemic treatment of WT mice with ERM (20 mg/kg body weight), as outlined in Figure 4A, substantially inhibited bone loss, as compared with ethanol control as well as relative to JSM and PC, which exhibited a modest protective effect in comparison with ethanol control (Figure 4B). In stark contrast, ERM failed to inhibit bone loss in *Del1*$^{-/-}$ mice (Figure 4C). Consistent with our findings in WT mice exposed to LPS-induced lung injury (Figure 2, B and D; and Figure 3, C–E and H), treatment of WT mice with ERM (but not with the other antibiotics tested) suppressed neutrophil infiltration in the gingival tissue (Figure 4D) and inhibited gingival mRNA expression of *Il17* and *Il6*, while upregulating the expression of *Del1* and *Il10* mRNA (Figure 4E). In great contrast, in *Del1*$^{-/-}$ mice, ERM failed to suppress neutrophil infiltration (Figure 4F) or to regulate cytokine (IL-17, IL-6, IL-10) expression at the mRNA or protein level (Figure 4G). IHC analysis revealed that treatment with ERM (but not with JSM, PC, or ethanol control) rescued DEL-1 protein expression in the periodontal ligament of WT mice while causing a decrease in the numbers of elastase-positive cells in the same area (Figure 4H). Taken together with our earlier data from this study, ERM exerts protective DEL-1–dependent immunomodulatory effects in at least 2 mucosal inflammatory disease models.

ERM regulates the C/EBPβ transcription factor and reverses IL-17–induced suppression of DEL-1 expression. As shown in Figure 1, A and B, ERM upregulated DEL-1 expression in HMVECs. Moreover, ERM

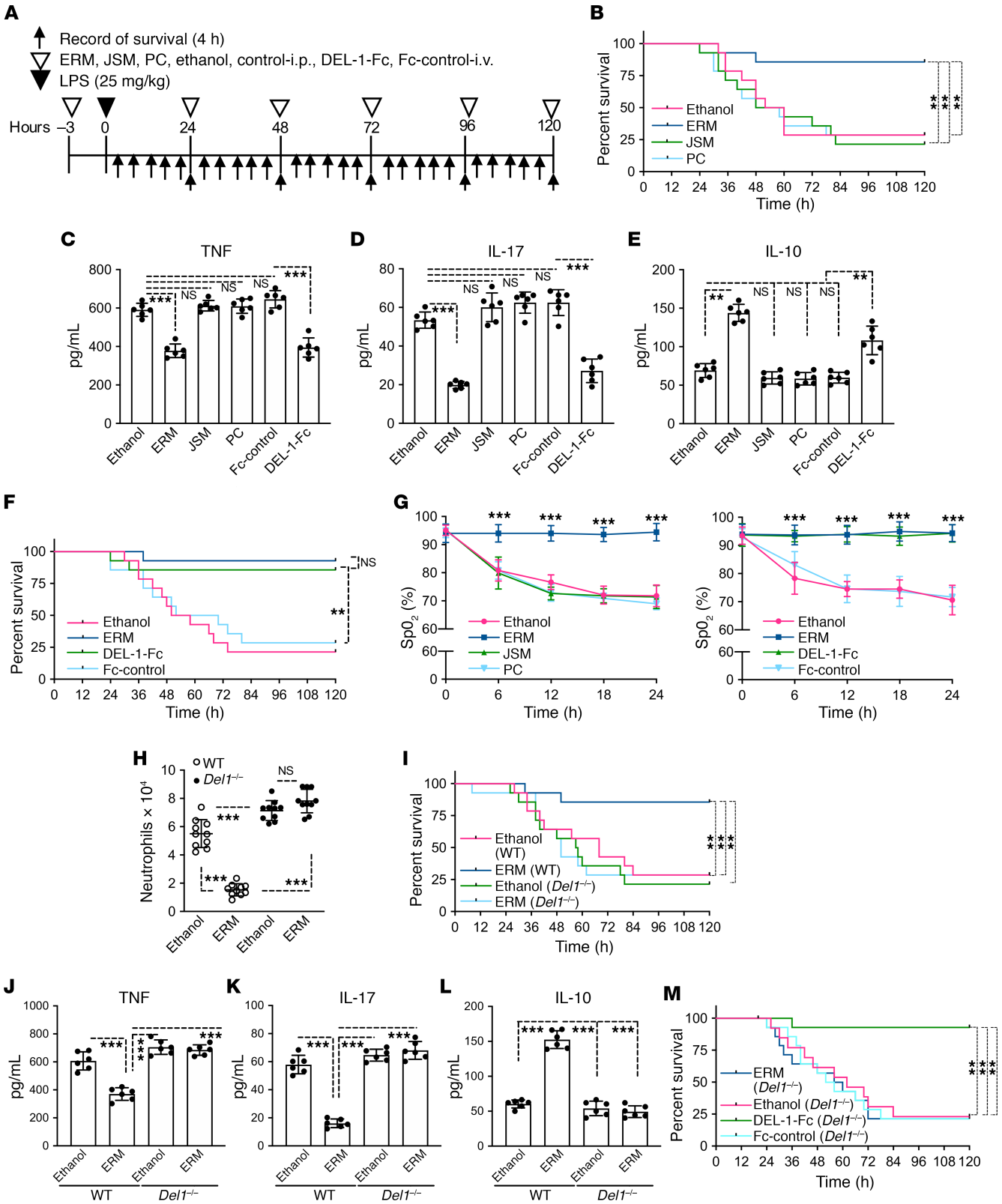

Figure 3. ERM improves mouse survival after LPS-induced acute lung injury in a manner comparable to that of DEL-1–Fc. (**A**) Experimental design. *E. coli* LPS (25 mg/kg; lethal dose) was administrated intratracheally. ERM, JSM, PC (all 3 antibiotics at 20 mg/kg), or ethanol control was administrated i.p., while DEL-1–Fc (10 μg) or Fc control (3.3 μg; equal molar amount with 10 μg DEL-1–Fc) was administered intravenously, at the indicated time points. (**B**) Survival rates for mice treated with ethanol control, ERM, JSM, or PC and subjected to acute lung injury by LPS (n = 14 mice/group). (**C**–**E**) Determination of TNF (**C**), IL-17 (**D**), and IL-10 (**E**) serum levels in LPS-challenged mice treated with ERM (or controls) or DEL-1–Fc (or Fc control); serum was collected 24 hours after LPS administration (n = 6 mice/group). (**F**) Survival rates of mice treated with DEL-1–Fc or Fc-control and subjected to acute lung injury by LPS (n = 14 mice/group). (**G**) Dynamics of oxygen saturation (SpO_2) levels in mice subjected to LPS-induced acute lung injury over the course of 24 hours

following LPS administration and treatment with the indicated antibiotics (left panel), DEL-1–Fc (right panel), or controls (ethanol or Fc) (n = 10 mice/group). (**H** and **I**) WT and *Del1*$^{-/-}$ mice were challenged with LPS and treated with ERM (or ethanol control) or DEL-1–Fc (or Fc control) as outlined in panel **A**. Neutrophil numbers were calculated in the BALF of WT and *Del1*$^{-/-}$ mice 24 hours after LPS administration (n = 10 mice/group) (**H**). Survival rate of WT and *Del1*$^{-/-}$ mice subjected to LPS-induced acute lung injury (n = 14 mice/group) (**I**). (**J**–**L**) Serum levels of TNF (**J**), IL-17 (**K**), and IL-10 (**L**) in LPS-challenged WT and *Del1*$^{-/-}$ mice treated with ERM (or ethanol control) or DEL-1–Fc (or Fc control); serum was collected 24 hours after LPS administration (n = 6 mice/group). (**M**) Survival rate of LPS-challenged *Del1*$^{-/-}$ mice treated with ERM (or ethanol control) or DEL-1–Fc (or Fc control) (n = 14 mice/group). Data are presented as the mean ± SD. $^{**}P < 0.01$ by the log-rank test (**B**, **F**, **I**, and **M**). $^{**}P < 0.01$, $^{***}P < 0.001$ by 1-way ANOVA followed by Tukey's multiple comparisons test (**C**, **D**, **E**, **H**, **J**, **K**, and **L**). $^{***}P < 0.001$ by 2-way ANOVA followed by Holm-Šidák multiple comparisons test (**G**).

promoted DEL-1 expression under in vivo inflammatory conditions in the lungs (Figure 2, D and G) and the periodontium (Figure 4, E and H). Because DEL-1 expression is inhibited by certain inflammatory cytokines, such as IL-17 (20), we reasoned that ERM can also reverse the downregulation of DEL-1 expression by IL-17. To this end, we examined *DEL1* gene expression in HMVECs stimulated with IL-17. ERM, but not JSM or PC, reversed the ability of IL-17 to inhibit DEL-1 expression, and in fact, ERM elevated *DEL1* expression over and above its constitutive levels (ethanol control treatment) (Figure 5A). In further experiments, we transfected HMVECs with a h*DEL1*-promoter-Luc-plasmid and treated them with ERM, JSM, PC or ethanol control. Consistent with our data in Figure 1, the *DEL1* promoter (luciferase) activity was significantly upregulated by ERM, but not by JSM or PC, relative to ethanol control (Figure 5B). Moreover, whereas IL-17 inhibited the *DEL1* luciferase activity in HMVECs, ERM reversed this inhibitory effect (Figure 5C). The transcription factor C/EBPβ is involved in the regulation of *DEL1* transcription, and its ability to bind to the *DEL1* (*EDIL3*) promoter is inhibited by IL-17 (20). We thus next investigated whether ERM promotes C/EBPβ binding to the *DEL1* promoter using a quantitative chromatin immunoprecipitation assay (ChIP-qPCR) (29). Our ChIP assay revealed that ERM, but not JSM or PC, enhanced the binding of C/EBPβ to the *DEL1* promoter (Figure 5D). Additionally, ERM not only reversed the inhibitory effect of IL-17 on C/EBPβ binding to the *DEL1* promoter but also elevated C/EBPβ binding over and above its constitutive level (ethanol control treatment) (Figure 5E). Taken together, ERM not only counteracts the inhibitory effect of IL-17 on the binding activity of C/EBPβ for the *DEL1* promoter, as previously shown for resolvins (20) and DHEA (29), but also can directly enhance the binding of C/EBPβ to the *DEL1* promoter.

ERM activates the GHSR/JAK2 signaling pathway to regulate DEL-1 expression. It was previously shown that ERM interacts with the GHSR, which is necessary for the ability of ERM to inhibit inflammatory responses in chondrocytes (30). To further explore the mechanism(s) whereby ERM upregulates DEL-1, we examined possible involvement of GHSR in DEL-1 regulation using ERM-treated HMVECs. First, using immunoblotting and immunofluorescence analysis, we showed that HMVECs express GHSR (Supplemental Figure 2). We next incubated HMVECs with ERM or ghrelin (a 28–amino acid peptide that functions as a natural endogenous ligand of GHSR, refs. 31, 32) and investigated the role of GHSR in *DEL1* gene expression. Both ERM and ghrelin significantly upregulated DEL-1 mRNA and protein expression (Figure 6A), and siRNA-mediated knockdown of *GHSR* (Supplemental Figure 2) abolished both ERM- and ghrelin-mediated DEL-1 upregulation (Figure 6A). These data show that the GHSR signaling pathway is involved in the induction of DEL-1 expression. We next investigated whether ghrelin can also suppress neutrophil infiltration in the lungs upon intratracheal challenge with a sublethal dose (2.5 mg/kg body weight) of LPS (Supplemental Figure 3A). First, in a dose-response study, we determined a dose of ghrelin capable of significantly upregulating *DEL1* mRNA expression in the lungs (Supplemental Figure 3B). Using ghrelin at 100 μg/kg (minimum concentration yielding maximum induction of *DEL1*; Supplemental Figure 3B), we showed that ghrelin suppressed neutrophil infiltration (Supplemental Figure 3C) and MPO activity in the BALF (Supplemental Figure 3D). Moreover, ghrelin inhibited the induction of proinflammatory cytokine (*Il6*, *Il17*, *Tnf*) expression and promoted the induction of *Del1* and *Il10* expression in the lungs (Supplemental Figure 3E). The antiinflammatory effects of ghrelin at 100 μg/kg were comparable to those of ERM at 20 mg/kg (Supplemental Figure 3, C–E). Taken together, GHSR signaling is required for ERM- and ghrelin-mediated DEL-1 upregulation; moreover, ghrelin-induced signaling reproduces the DEL-1–dependent antiinflammatory effects of ERM. Subsequently, we investigated the GHSR-mediated intracellular pathway that drives DEL-1 expression.

Activation of GHSR was shown to modulate JAK2-associated PI3K and AKT phosphorylation as well as MAPK signaling (33–36). Moreover, AKT signaling induces Ser9 phosphorylation of GSK3β, which is involved in the regulation of *DEL1* transcription (20). Consistent with those reports, ERM

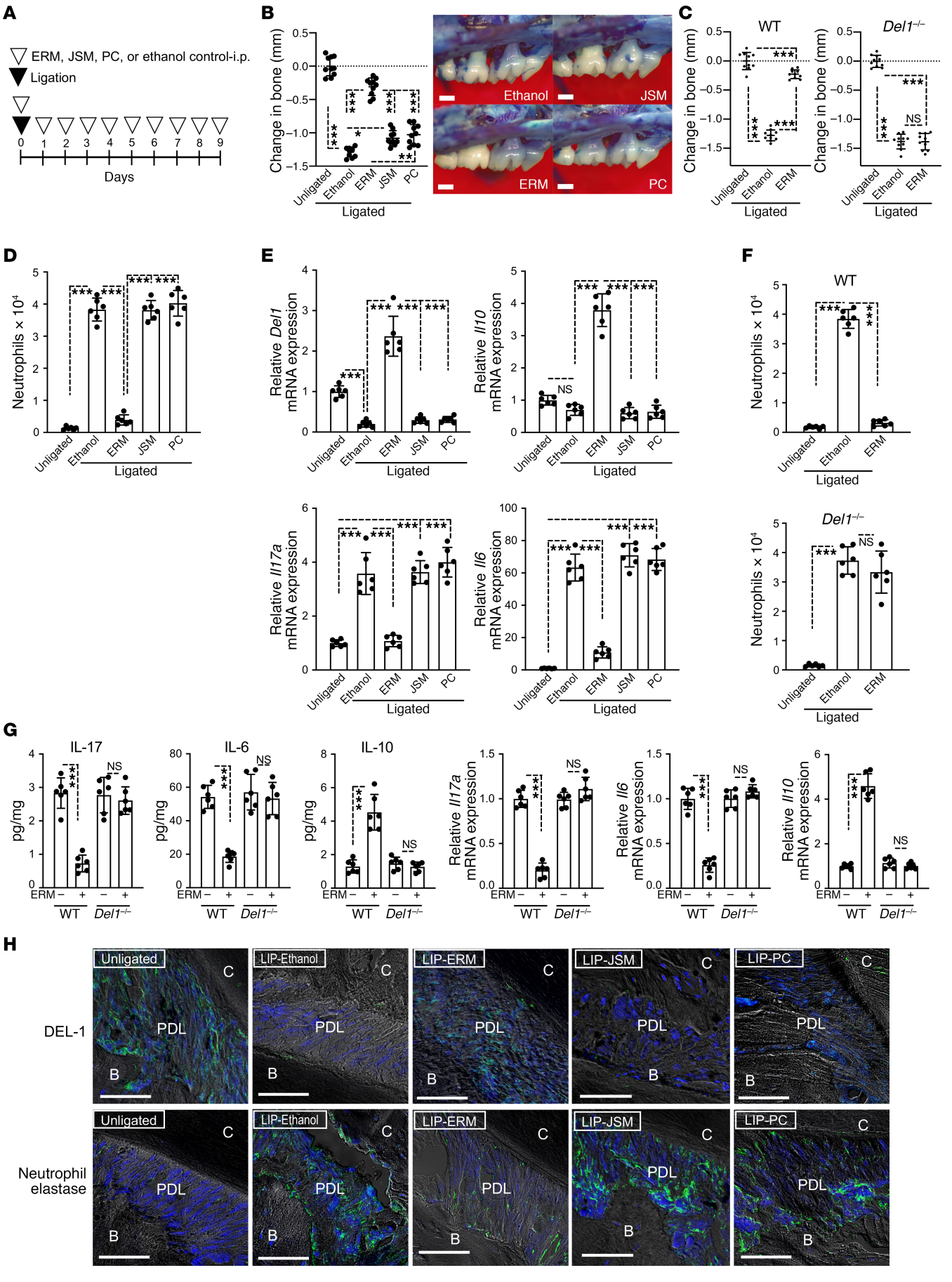
A
ERM, JSM, PC, or ethanol control-i.p.
Ligation
0 1 2 3 4 5 6 7 8 9
Days
B
Change in bone (mm)
Unligated Ethanol ERM JSM PC
Ligated
Ethanol
JSM
ERM
PC
C
WT
Del1−/−
Change in bone (mm)
NS
Unligated Ethanol ERM
Ligated
D
Neutrophils × 10⁴
Unligated Ethanol ERM JSM PC
Ligated
E
Relative Del1 mRNA expression
Relative Il10 mRNA expression
Relative Il17a mRNA expression
Relative Il6 mRNA expression
F
WT
Del1−/−
Neutrophils × 10⁴
G
IL-17
IL-6
IL-10
pg/mg
Relative Il17a mRNA expression
Relative Il6 mRNA expression
Relative Il10 mRNA expression
ERM
WT
Del1−/−
H
DEL-1
Neutrophil elastase
Unligated
LIP-Ethanol
LIP-ERM
LIP-JSM
LIP-PC
C
PDL
B

Figure 4. ERM suppresses ligature-induced inflammatory bone loss in a DEL-1–dependent manner. (**A**) Experimental design. Periodontal bone loss was induced in WT or *Del1*$^{-/-}$ mice for 9 days by ligating a maxillary second molar and leaving the contralateral tooth unligated (baseline control). Groups of mice were given ERM (20 mg/kg), JSM (20 mg/kg), PC (20 mg/kg), or ethanol control i.p. every day until the day before sacrifice (day 8). (**B**) Measurements of bone loss in the indicated groups of LIP-subjected mice (left panel; *n* = 10 mice/group) and representative images of maxillae from each group (right panel). (**C**) Bone loss was measured in littermate WT or *Del1*$^{-/-}$ mice that were subjected to LIP and treated with ERM (20 mg/kg) or ethanol control as shown in panel **A** (*n* = 10 mice/group). (**D**) Numbers of neutrophils in the gingiva of LIP-subjected WT mice treated with ethanol control, ERM (20 mg/kg), JSM (20 mg/kg), or PC (20 mg/kg) as described above (*n* = 6 mice/group). (**E**) Relative mRNA expression of the indicated molecules in the gingival tissue from LIP-subjected WT mice treated with ERM, JSM, PC, or ethanol control as above. Data were normalized to *Gapdh* mRNA and are presented as fold change relative to baseline (unligated control), which was set as 1 (*n* = 6 mice/group). (**F**) Numbers of neutrophils in the gingival tissue of LIP-subjected WT or *Del1*$^{-/-}$ mice treated with ERM (20 mg/kg) or ethanol control (*n* = 6 mice/group). (**G**) Determination of the protein and mRNA levels of IL-17, IL-6, and IL-10 in the gingival tissue of LIP-subjected WT or *Del1*$^{-/-}$ mice, which were treated (or not; ethanol control) with 20 mg/kg ERM as outlined in panel **A**. Protein concentrations (pg cytokines/mg total protein in tissue lysates are shown) and mRNA expression were determined by ELISA and qPCR, respectively. The mRNA data were normalized to *Gapdh* mRNA and are presented as fold change relative to vehicle-treated WT mice, which was set as 1 (*n* = 6 mice/group). (**H**) Tissue sections from LIP-subjected WT mice were stained for DEL-1, neutrophil elastase and nuclei using DAPI. Scale bars, 100 μm. Data are presented as the mean ± SD. $^{*}P < 0.01$, $^{***}P < 0.0001$ by 1-way ANOVA followed by Tukey's multiple comparisons test (**B**–**G**).

induced phosphorylation of JAK2, AKT, GSK3β, and MAPK p38 in HMVECs, whereas *GHSR* knockdown reduced these ERM-induced phosphorylation events (Figure 6B). To evaluate which of these signaling molecules are important for DEL-1 induction, HMVECs were pretreated with inhibitors of JAK2, AKT, or MAPK p38. Inhibitors of JAK2 and MAPK p38 (AG490 and SB203580, respectively), but not an inhibitor of PI3K/AKT signaling (LY294002), blocked ERM-mediated upregulation of *DEL1* mRNA expression (Figure 6C), *DEL1* promoter/luciferase activity (Figure 6D), as well as C/EBPβ binding to the *DEL1* promoter (Figure 6E). Thus, JAK2 and MAPK p38, but not PI3K or AKT, mediate the direct effect of ERM on DEL-1 upregulation in HMVECs.

We next examined whether ERM-induced activation (phosphorylation) of AKT is required for the ability of ERM to reverse the inhibitory effect of IL-17 on DEL-1 expression. The rationale for this experiment was that the proresolving lipid mediator resolving D1 (RvD1) causes AKT-induced GSK3β phosphorylation on Ser9, which in turn antagonizes the GSK3β-dependent inhibitory effect of IL-17 on *DEL1* transcription (20). Regardless of the absence or presence of IL-17, ERM upregulated *DEL1* mRNA expression (Figure 6, C and F), *DEL1* promoter/luciferase activity (Figure 6, D and G), and the binding of C/EBPβ to the *DEL1* promoter (Figure 6, E and H), as compared with the constitutive levels of these activities in the ethanol control group. All these activities were inhibited by AG490 (Figure 6, C–H), suggesting that JAK2 regulates both the induction of DEL-1 expression by ERM as well as the ability of ERM to reverse the inhibitory effect of IL-17 on DEL-1 expression. In the absence of IL-17, RvD1 did not upregulate any of these activities as compared with the ethanol control treatment (Figure 6, F–H); however, RvD1 reversed the inhibitory effects of IL-17 on *DEL1* mRNA expression (Figure 6F), *DEL1* promoter/luciferase activity (Figure 6G), and C/EBPβ binding to the *DEL1* promoter (Figure 6H), thereby restoring these activities to levels similar to those seen in the ethanol control group. Inhibition of AKT signaling by LY249002 suppressed the ability of both ERM and RvD1 to counteract the inhibitory effect of IL-17 on *DEL1* expression (Figure 6F). In contrast to LY249002, AG490 (JAK2 inhibitor) and SB203580 (MAPK p38 inhibitor) did not affect the ability of RvD1 to reverse the IL-17–inhibitory effect on *DEL1* expression (Figure 6F), *DEL1* promoter/luciferase activity (Figure 6G), or C/EBPβ binding to the *DEL1* promoter (Figure 6H).

These above-described data suggest that JAK2 and MAPK p38 are unique to the ERM-induced pathway and are unlikely to be activated by RvD1 in HMVECs. To further substantiate this notion, we investigated possible differences between the ERM- and RvD1-induced signaling pathways. Both ERM and RvD1 induced Ser473 phosphorylation of AKT and Ser9 phosphorylation of GSK3β; however, ERM, but not RvD1, induced the phosphorylation of JAK2 and MAPK p38 (Figure 6I). Importantly, the JAK2 inhibitor AG490 inhibited ERM-induced phosphorylation of AKT and GSK3β (Figure 6I), suggesting that the latter 2 signaling molecules are activated downstream of JAK2 phosphorylation by ERM. These data suggest that ERM activates PI3K/AKT signaling via JAK2, whereas RvD1 activates PI3K/AKT in a JAK2-independent manner. Taken together, these data in HMVECs show that ERM shares an AKT-GSK3β pathway with RvD1 responsible for reversing the inhibitory effect of IL-17 on DEL-1 expression; however, ERM also activates another JAK2-dependent pathway, which is not shared by RvD1, which depends on MAPK p38 and can directly induce DEL-1 expression.

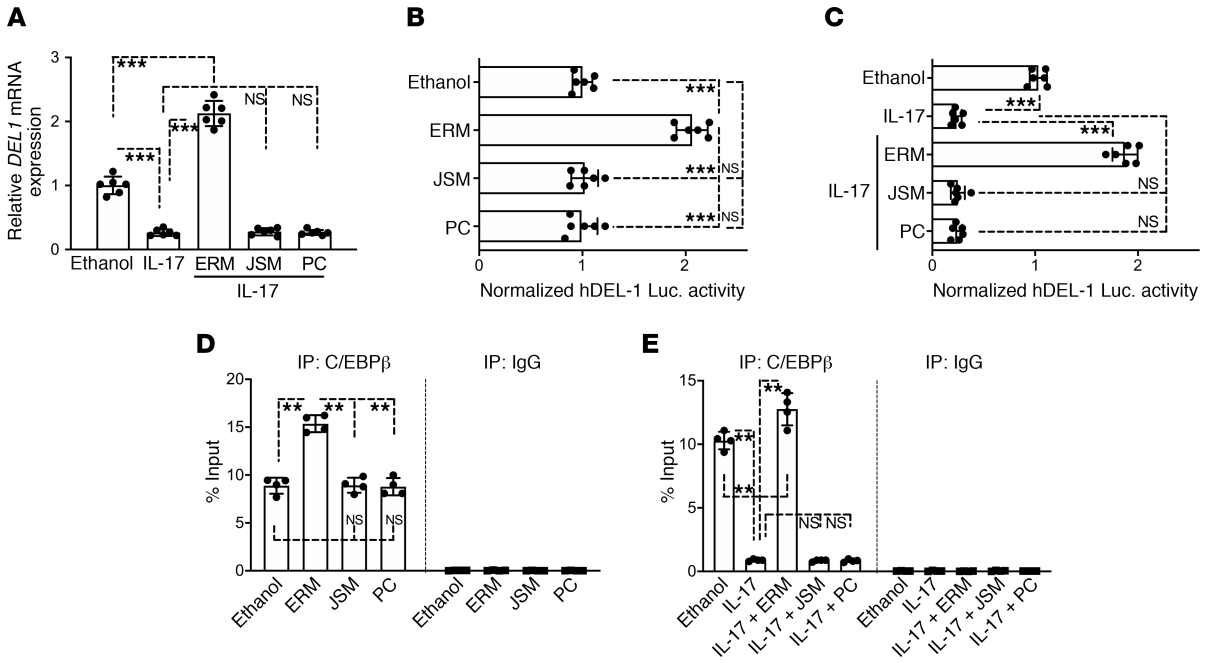

Figure 5. ERM reverses IL-17–mediated suppression of DEL-1 by regulating the C/EBPβ transcription factor. (**A**) HMVECs were stimulated as indicated for 4 hours in the absence or presence of IL-17 (5 ng/mL). Prior to IL-17 stimulation, the cells were pretreated for 30 minutes with ERM (10 μg/mL), JSM (10 μg/mL), or PC (10 μg/mL). *DEL1* mRNA expression was determined by qPCR, and data were normalized against *GAPDH* mRNA and expressed as fold induction relative to ethanol treatment (vehicle control), which was assigned an average value of 1 (n = 6 sets of cultures/group). (**B** and **C**) HMVECs were transiently transfected with hEDIL3-promoter-Luc reporter plasmid, pretreated for 30 minutes with or without ERM (10 μg/mL), JSM (10 μg/mL), or PC (10 μg/mL), followed by 8-hour stimulation with or without IL-17 (5 ng/mL), and analyzed for luciferase activity. A Renilla luciferase construct was cotransfected as an internal control for normalization. Data are presented as fold change relative to ethanol control treatment, which was set as 1 (n = 6 sets of cultures/group). (**D**) ChIP analysis of C/EBPβ occupancy at the *DEL1* promoter in HMVECs treated for 4 hours with ethanol control, ERM (10 μg/m), JSM (10 μg/m), or PC (10 μg/m) (n = 4 sets of cultures/group). (**E**) Same experimental setup as in panel **D**, with included stimulation with IL-17 (5 ng/mL) for 4 hours following 30 minutes' pretreatment with ERM and controls (n = 4 sets of cultures/group). Nonimmunoprecipitated cell extracts were used as input samples. In the experiments whose results are shown in **A**, **C**, and **E**, sequential treatments were performed without intermediate washing steps. Data are expressed as percentage of input. Data are presented as the mean ± SD. $^{**}P < 0.001$, $^{***}P < 0.0001$ by 1-way ANOVA followed by Tukey's multiple comparisons test.

Discussion

Macrolides are frequently used as antibiotics to treat respiratory infections and noninfectious pulmonary disease. Macrolides have strong tissue penetration ability compared with other antibiotics, leading to tissue concentrations that often exceed the serum concentrations (37). In addition to their antibiotic activities, macrolides have immunomodulatory properties that are useful for the treatment of chronic inflammatory diseases at mucosal barrier sites, including the lungs (2, 9, 38–40). However, little is known on the immunomodulatory mechanisms of macrolides. In this study, we focused on the 14-membered ring macrolide ERM and obtained important insights on its immunomodulatory action and its underlying mechanisms. ERM upregulated DEL-1 mRNA and protein levels in cultured HMVECs, as well as in vivo, at 2 mucosal sites, the lungs and the periodontium. Consistent with the anti–neutrophil recruitment action of endothelial cell–derived DEL-1 (14, 15), ERM suppressed neutrophil infiltration in BALF and the periodontium in a DEL-1–dependent manner. The biological significance of this mechanism was demonstrated by the protective actions of ERM against lethal pulmonary inflammation and inflammatory bone loss in models of LPS-induced acute lung injury and LIP, respectively. ERM failed to confer protection in the absence of endogenous DEL-1. We have moreover demonstrated that ERM modulates DEL-1 expression by activating GHSR/JAK2 signaling, which is a novel pathway for the regulation of C/EBPβ, a critical transcription factor for *DEL1* gene transcription (20).

We have previously shown that DEL-1 expression is severely reduced under inflammatory conditions (15, 20, 29). Specifically, both IL-17 and TNF diminish DEL-1 expression by targeting C/EBPβ, although their effects are reversed by the proresolving lipid mediator RvD1 and steroid hormone dehydroepiandrosterone (DHEA) (20, 29). Although RvD1 and DHEA use different receptors (GPR32 and/or ALX/FPR2 vs. TrkA, respectively), they both activate PI3K/AKT signaling to restore C/EBPβ binding to the *DEL1* promoter region, thereby counteracting the inhibitory effect of inflammatory cytokines on DEL-1 production.

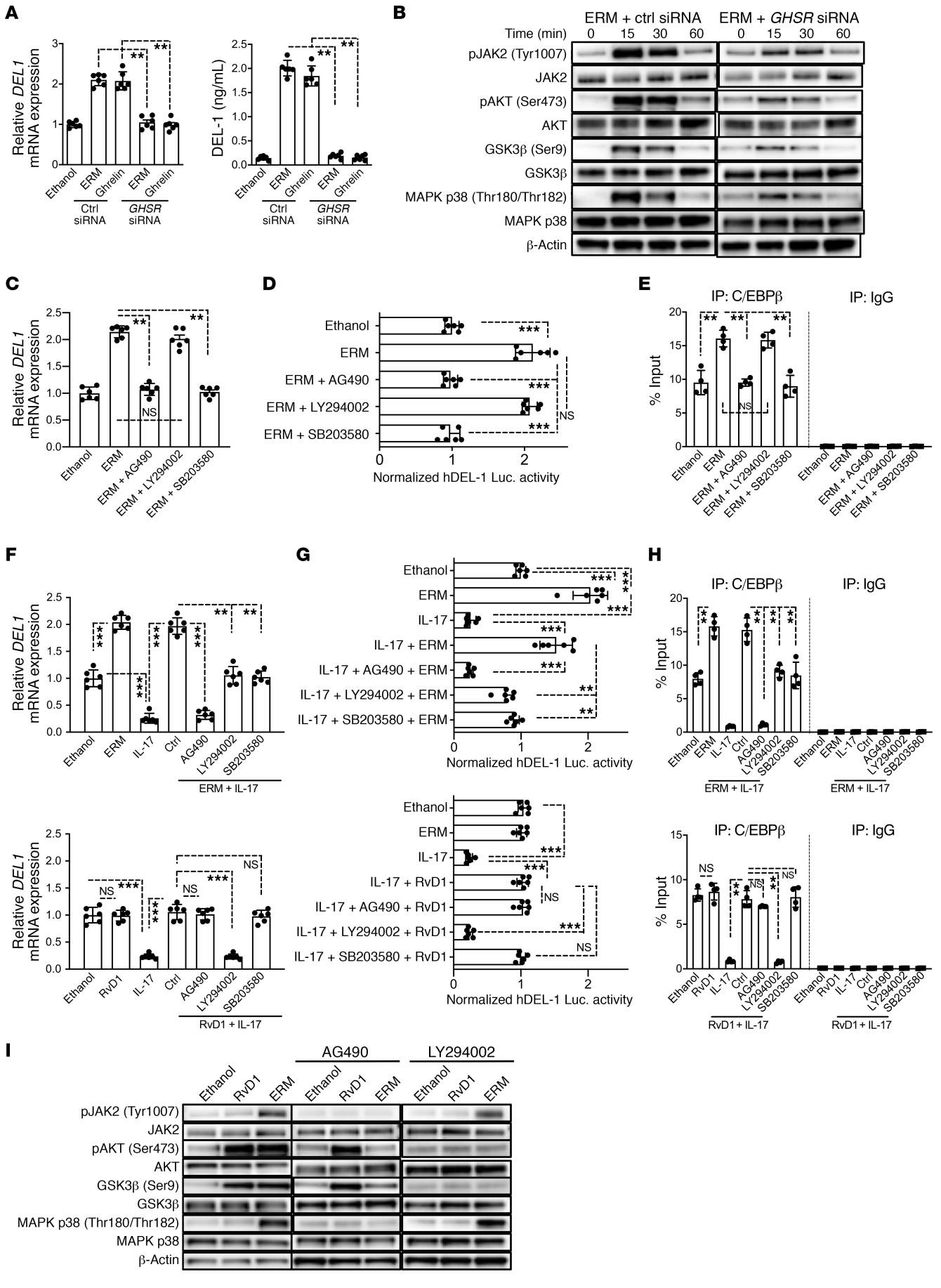
A
Relative DEL1 mRNA expression
DEL-1 (ng/mL)
Ethanol
ERM
Ghrelin
ERM
Ghrelin
Ctrl siRNA
GHSR siRNA
B
ERM + ctrl siRNA
ERM + GHSR siRNA
Time (min)
0 15 30 60 0 15 30 60
pJAK2 (Tyr1007)
JAK2
pAKT (Ser473)
AKT
GSK3β (Ser9)
GSK3β
MAPK p38 (Thr180/Thr182)
MAPK p38
β-Actin
C
Relative DEL1 mRNA expression
Ethanol
ERM
ERM + AG490
ERM + LY294002
ERM + SB203580
NS
D
Ethanol
ERM
ERM + AG490
ERM + LY294002
ERM + SB203580
NS
Normalized hDEL-1 Luc. activity
E
IP: C/EBPβ
IP: IgG
% Input
NS
F
Relative DEL1 mRNA expression
Ethanol
ERM
IL-17
Ctrl
AG490
LY294002
SB203580
ERM + IL-17
Ethanol
RvD1
IL-17
Ctrl
AG490
LY294002
SB203580
RvD1 + IL-17
G
Ethanol
ERM
IL-17
IL-17 + ERM
IL-17 + AG490 + ERM
IL-17 + LY294002 + ERM
IL-17 + SB203580 + ERM
Normalized hDEL-1 Luc. activity
Ethanol
ERM
IL-17
IL-17 + RvD1
IL-17 + AG490 + RvD1
IL-17 + LY294002 + RvD1
IL-17 + SB203580 + RvD1
NS
Normalized hDEL-1 Luc. activity
H
IP: C/EBPβ
IP: IgG
% Input
ERM + IL-17
RvD1 + IL-17
I
AG490
LY294002
Ethanol
RvD1
ERM
pJAK2 (Tyr1007)
JAK2
pAKT (Ser473)
AKT
GSK3β (Ser9)
GSK3β
MAPK p38 (Thr180/Thr182)
MAPK p38
β-Actin

Figure 6. ERM activates GHSR/JAK2 signaling for regulating DEL-1 expression. (**A**) *DEL1* mRNA expression determined by qPCR and DEL-1 protein levels determined by ELISA in control or *GHSR* siRNA-transfected HMVECs treated with ERM (10 μg/mL) or ghrelin (5 μg/mL) 3 hours (mRNA) or 6 hours (protein) (n = 6 culture sets/group). Data normalized against *GAPDH* mRNA are expressed as fold induction relative to ethanol (set as 1). (**B**) HMVECs, pretreated for 24 hours with control or *GHSR* siRNA (20 nM), were incubated with ERM and assayed for phosphorylation at indicated points. (**C**) After 1-hour pretreatment with AG490 (10 μM), LY294002 (20 μM), or SB203580 (10 μM), HMVECs were incubated 3 hours with ERM and assayed for *DEL1* expression (n = 6 culture sets/group). Data normalized against *GAPDH* mRNA were expressed as fold induction relative to ethanol control (set as 1). (**D**) HMVECs were transiently transfected with hEDIL3-promoter-Luc reporter plasmid, pretreated 1 hour with inhibitors, and subsequently incubated 8 hours with ERM or control followed by luciferase assay. Data are presented as fold change relative to ethanol control, set as 1 (n = 6 culture sets/group). (**E**) HMVECs, pretreated as above with inhibitors, were incubated 4 hours with ERM and subjected to ChIP analysis of C/EBPβ occupancy at the EDIL3 promoter (n = 4 culture sets/group). (**F**) After 30-minute pretreatment with ERM or RvD1 (100 nM), HMVECs were stimulated (3 hours), or not, with IL-17 (5 ng/mL). *DEL1* mRNA expression was assayed and presented as above (n = 6 HMVEC culture sets/group). (**G**) HMVECs were transiently transfected with hEDIL3-promoter-Luc reporter plasmid and pretreated with inhibitors. After 1 hour, the cells were treated with ERM, RvD1, or control for 30 minutes, followed by 8-hour stimulation with IL-17 and luciferase activity assay (n = 6 culture sets/group). Data are presented as fold change relative to ethanol (set as 1). (**H**) After 1-hour pretreatment with inhibitors, HMVECs were treated with ERM, RvD1, or ethanol for 30 minutes, followed by 4-hour stimulation with IL-17. Chromatin was immunoprecipitated with anti–C/EBPβ IgG and subjected to qPCR of the *DEL1* promoter. Nonimmunoprecipitated cell extracts served as input samples. (**I**) After 1-hour pretreatment with inhibitors, HMVECs were incubated with RvD1 or ERM for 30 minutes and assayed for phosphorylation. In experiments shown in **A**–**I**, sequential treatments were performed without intermediate washing steps. Each compound was used at the same concentration in all experiments. Data are shown as means ± SD. $^{**}P < 0.001$, $^{***}P < 0.0001$ by 1-way ANOVA with Tukey's multiple comparisons test (**A** and **C**–**H**).

ERM shares a similar function with RvD1 and DHEA, in that ERM can also reverse inflammation-induced downregulation of DEL-1 transcription in a PI3K/AKT-dependent manner. However, what is unique and novel about ERM is that it can directly upregulate DEL-1 expression even under normal homeostatic (noninflammatory) conditions; RvD1 and DHEA cannot directly induce DEL-1 expression (20, 29). Thus, ERM not only counteracts the inhibitory effect of inflammation on the promoter binding activity of C/EBPβ ("reversal effect"), as we showed earlier for RvD1 (20) and DHEA (29), but also can directly enhance the binding of C/EBPβ to the *DEL1* promoter.

Besides activating GHSR/JAK2-dependent PI3K/AKT signaling, which drives the reversal effect, ERM activates a pathway that is not shared by RvD1 but that can directly induce DEL-1 expression. This unique pathway depends on MAPK p38 because this kinase is activated by ERM in a JAK2-dependent manner, and importantly, pharmacological inhibition of MAPK p38 completely inhibited the ability of ERM to (a) promote the binding of C/EBPβ to the *DEL1* promoter region, (b) stimulate *DEL1* promoter/luciferase activity, and (c) induce *DEL1* mRNA expression. Thus, JAK2 is an essential component of ERM-induced signaling, which bifurcates and leads to MAPK p38-dependent DEL-1 expression and AKT-dependent reversal of the IL-17/GSK3β inhibitory effect on DEL-1 expression.

In line with the finding that GHSR was required for the ability of ERM to upregulate DEL-1, ghrelin also enhanced DEL-1 expression and exerted a similar antiinflammatory effect as ERM in the lungs after intratracheal challenge with a sublethal dose of LPS. Similar to DEL-1, which is a potent antagonist of IL-17 induction (13, 17, 18, 20, 21), ghrelin was earlier shown to inhibit IL-17 responses (41, 42). Future studies are warranted for a better understanding of the potential relationship between DEL-1 and ghrelin in regulating IL-17 responses and how they might antagonize leptin, which promotes Th17 differentiation and IL-17 production (42, 43).

Severe periodontitis affects approximately 10% of adults, is associated with increased risk of certain systemic disorders (e.g., atherosclerosis and rheumatoid arthritis), and remains a serious public health and economic burden (27, 44–46). This oral disease is driven by IL-17 in both mice and humans (17, 28), and DEL-1 is a strong inhibitor of IL-17–driven immunopathology in periodontitis and other disease models in mice as well as nonhuman primates (17, 18, 21, 47). Our potentially novel discovery that ERM both upregulates DEL-1 and prevents its downregulation by inflammatory stimuli offers a new approach to the treatment of periodontitis in humans. Although the protective effect of ERM against ligature-induced periodontal bone loss might, in part, be contributed by its antibiotic activity, such contribution should be minimal, as shown by the weak protective effects of either JSM or PC in the same model. Moreover, if the protective effect of ERM against bone loss were substantially dependent on its antibiotic action, then ERM should have exhibited a measurable protective effect against bone loss in *Del1*-deficient mice. We therefore conclude that ERM protects against experimental periodontitis predominantly through its DEL-1–dependent antiinflammatory action. In addition to its antiinflammatory effects, DEL-1 was recently shown to have osteogenic activity and to promote periodontal bone regeneration (48), suggesting that ERM may also find an application in regenerative medicine.

The pathogenesis of acute lung injury is characterized by lung epithelial integrity disruption and infiltration of neutrophils into the lungs, leading to interstitial edema and alveolar collapse (49). By secreting

cytokines and other inflammatory mediators, neutrophils may be important effectors in acute lung injury (50). Recently, clarithromycin (CAM), also a 14-membered macrolide, was found to modulate the immunosuppressive $CD11b^{+}Gr\text{-}1^{+}$ cell population, thereby ameliorating lethal endotoxic shock and postinfluenza bacterial pneumonia (51). In that study, the authors showed that clarithromycin-induced $CD11b^{+}Gr\text{-}1^{+}$ cells protected mice against LPS-induced lethality by increasing IL-10 expression. Whether CAM can mediate any of its immunomodulatory action through regulatory effects on DEL-1 expression in the lungs is currently uncertain. However, the immunomodulatory effects may vary between different macrolides. For instance, in vitro studies have suggested that CAM has lower immunomodulatory activity as compared with the 14-membered macrolide roxithromycin (52). Moreover, CAM displayed a significantly weaker effect in reducing IL-6 production by human macrophages as compared with ERM (53). Previous studies have suggested that 14- and 15-membered, but not 16-membered macrolides, can inhibit the production of proinflammatory cytokines and chemokines in vivo and in vitro in isolated cells, including innate immune, epithelial, and endothelial cells (1, 54–56). Consistently, 16-membered JSM did not induce DEL-1 expression in vivo or in vitro.

Interestingly, in the sputum of patients with COPD, ERM led to a significant decrease in the total cell and neutrophil counts, inhibited neutrophil chemotaxis, and decreased the concentration of neutrophil elastase (57, 58). Our study showed that ERM, albeit not JSM or PC, induced IL-10 and decreased TNF and IL-17. Importantly, a recent study showed that anti–IL-17 pretreatment protects mice from the acute lung injury (59). These antiinflammatory effects of ERM are dependent on DEL-1 and, at least in part, on its anti–neutrophil recruitment action. In this regard, we have recently linked DEL-1's anti–leukocyte recruitment function to endothelial cell–derived DEL-1 and its ability to resolve tissue inflammation to macrophage-derived DEL-1 (14). Specifically, macrophage-derived DEL-1 regulates efferocytosis and the plastic reprogramming of macrophages to a proresolving phenotype with enhanced expression of antiinflammatory factors, such as TGF-β and resolvins, both of which can inhibit IL-17 and other proinflammatory cytokines (14).

Ghrelin has close structural identity with motilin (60, 61). ERM was shown to activate the motilin receptor, which has 52% overall amino acid identity with GHSR, suggesting that ERM could also act as a ghrelin receptor agonist (62). A subsequent study showed that ERM indeed acts through GHSR (30). Moreover, several studies have shown that certain immunomodulatory activities of ERM are mediated by GHSR (30, 63). GHSR is known as the ghrelin receptor involved in mediating growth hormone release and body weight increase, regulating gastrointestinal motility and secretion (60, 64, 65). The functions of GHSR also include attenuation of proinflammatory responses and regulation of immune functions related to aging and homeostasis (66) as well as cell protection in the cardiovascular system (67). Beneficial effects of ERM and ghrelin on local inflammation have also been reported (30). Our study is consistent with the findings linking ERM to GHSR-dependent antiinflammatory effects but additionally has provided novel insights into the immunomodulatory mechanisms of ERM. We demonstrated for the first time to our knowledge that the antiinflammatory effect of ERM depends on DEL-1, which is regulated downstream of GHSR signaling. We established an ERM-JAK2-MAPK p38 axis, which upregulates the constitutive expression of DEL-1, and an ERM-JAK2-PI3K-AKT-GSK3β axis, which reverses the inhibitory effect of IL-17 on DEL-1 expression. In contrast to ERM, JSM and PC had no protective role in the LPS-induced acute lung injury model but displayed a modest protective effect in the experimental periodontitis model; this is perhaps due to antibiotic action against periodontal bacterial species contributing to the induction of the host inflammatory response. Although we cannot formally exclude the possibility that the antibiotic action of ERM contributed to its protective effects in experimental periodontitis, such contribution is likely minimal (if any), since ERM failed to protect *Del1*$^{-/-}$ mice from inflammatory bone loss.

Importantly, DEL-1 production is progressively decreased with aging in both mice and humans, correlating with increased periodontal disease activity (17, 47, 68), and perhaps other inflammatory disorders, such as multiple sclerosis, where DEL-1 plays a major role (18). Therefore, the ability of ERM to upregulate DEL-1 expression may lead to a key novel approach for the treatment of aging-related inflammatory disorders. In conclusion, in vivo and in vitro evidence suggested that ERM exerts its immunomodulatory effects by regulating the local homeostatic factor DEL-1. Because DEL-1 is a strong inhibitor of IL-17–driven immunopathology (13), our study supports the use of ERM as an immunomodulatory agent for treating IL-17–driven inflammatory diseases at mucosal barrier sites.

Methods

Mice. Male WT C57BL/6N mice (10–12 weeks old) were purchased from Nihon CLEA (Tokyo, Japan). C57BL/6N *Del1*$^{-/-}$ mice were generated by Setsuro Tech (Tokushima, Japan) using GEEP methods (22, 23). CRISPR RNA was designed (*Del1* up CRISPR RNA [crRNA]: CTGGCTTTGGGCGCCCCCGG; protospacer adjacent motif [PAM]:CGG; *Del1* down crRNA: GGGGTGCCCCAGTTCGGCAA; PAM:AGG) as described by Choi et al. (15). Mice were maintained in individually ventilated cages and provided sterile food and water ad libitum under specific pathogen–free conditions.

Reagents. Recombinant human or mouse IL-17A was purchased from R&D Systems, Bio-Techne (Minneapolis, Minnesota, USA). The D-series resolvin RvD1 was purchased from Cayman Chemical (Ann Arbor, Michigan, USA). LY294002 (PI3K/AKT inhibitor) and SB203580 (MAPK p38 inhibitor) were purchased from MilliporeSigma (St. Louis, Missouri, USA). AG490 (JAK2 inhibitor) was purchased from InvivoGen (San Diego, California, USA). Rabbit polyclonal antibody against DEL-1 was from Proteintech (12480-1–AP; Rosemont, Illinois, USA). Rabbit monoclonal antibody (mAb) against β-actin (4970; clone 13E5), rabbit IgG antibodies against total AKT (9272; phosphorylation state independent), phospho-AKT (4060; clone D9E; Ser473), total JAK2 (3230; clone D2E12), phospho-JAK2 (3771; Tyr1007/1008), total GSK-3β (9315; clone 27C10), phospho-GSK3β (9336; Ser9), total MAPK p38 (9212), and phospho-MAPK p38 (9211) were purchased from Cell Signaling Technology (Danvers, Massachusetts, USA). Rabbit IgG antibodies against GHSR (H00002693-K) were from Abnova (Taipei City, Taiwan).

LPS-induced acute lung injury. LPS-induced acute lung injury was performed in *Del1*$^{-/-}$ mice and *Del1*$^{+/+}$ (WT) littermate controls using both sublethal (2.5 mg/kg body weight) and lethal (25 mg/kg body weight) doses of LPS in the presence or absence of ERM and control treatments, according to the experimental designs shown in Figure 2A and Figure 3A. Mice were anesthetized and were administered LPS (from *E. coli* 0111:B4; InvivoGen) intratracheally using MicroSprayer aerolizer (Penn-Centrury, Wyndmoor, Pennsylvania, USA). For treatment, ERM (20 mg/kg; Thermo Fisher Scientific, Waltham, Massachusetts, USA), JSM (20 mg/kg; FUJIFILM Wako Pure Chemical Corporation, Tokyo, Japan), PC (20 mg/kg; FUJIFILM Wako Pure Chemical Corporation), or ghrelin (100 μg/kg; Phoenix Pharmaceuticals, Burlingame, California, USA) were intraperitoneally injected into the mice. The concentration of ERM used was within the range of human plasma concentrations achieved with typical therapeutic activity of ERM (69). Ethanol served as vehicle control. The mice were sacrificed, and then bronchoalveolar lavage was collected as previously described (70, 71). MPO activity in BALF was measured based on the change in optical density at 450 nm resulting from oxidation of *o*-dianisidine dihydrochloride (72). Protein concentrations in tissue extracts were determined using the bicinchoninic acid microassay method (Thermo Fisher Scientific). Human DEL-1 was generated and purified as a fusion protein with the human IgG-Fc fragment as described previously (16, 47).

LIP model. A 5-0 silk ligature was tied around the maxillary left second molar, and the mice were euthanized 9 days after placement of the ligatures (73). The contralateral molar tooth in each mouse was left unligated (baseline control for bone loss measurements). Periodontal bone loss was assessed morphometrically in defleshed maxillae using a dissecting microscope (×40) fitted with a video image measurement system (Nikon Instruments, Tokyo, Japan). Specifically, the cementoenamel junction to the alveolar bone crest (CEJ-ABC) distance was measured on 6 predetermined points on the ligated second molar and the affected adjacent regions (73). Bone loss was calculated by subtracting the 6-site total CEJ-ABC distance for the ligated side of each mouse from the 6-site total CEJ-ABC distance of the contralateral unligated side. Negative values (in millimeters) indicated bone loss relative to the baseline (unligated control). LIP-subjected mice were intraperitoneally treated with ERM and control antibiotics using the doses mentioned above (*LPS-induced acute lung injury*) and according to the experimental design shown in Figure 4A.

Cell preparation, culture, and treatments. HMVECs (Lonza Japan, Chiba, Japan) were cultured on 2% gelatin-coated plates in Microvascular Endothelial Cell Growth Medium-2 (EGM-2MV; Lonza Japan) at 37°C and 5% CO_2. In all experiments, sequential treatments were performed without intermediate washing steps.

ChIP assay followed by qPCR. ChIP analysis of C/EBPβ binding to the *DEL1* promoter was performed in HMVECs as previously reported (20, 29) using the SimpleChIP Plus Enzymatic Chromatin IP Kit with magnetic beads (Cell Signaling Technology) following the manufacturer's instructions. Briefly, cross-linked chromatin was immunoprecipitated with nonimmune rabbit IgG (Cell Signaling Technology) or rabbit IgG mAb against anti–histone H3 (D2B12; Cell Signaling Technology) or rabbit IgG antibody against C/EBPβ (C19 sc-150; Santa Cruz Biotechnology, Dallas, Texas, USA). For PCR, primers 5′ CTTATAGCAGAAGGAGCTGAAAGAG 3′ and 5′ TGGAGAACAATGAAGGCGTGAG 3′ flanking 2 putative C/EBPβ

binding sites in the *DEL1* promoter (−328 to −589 base pairs) were used. ChIP-qPCR data obtained with the C/EBPβ antibody or nonimmune IgG were normalized using the percentage input method that normalizes to chromatin input based on following equation: % input = $100 \times 2^{Ct[adjusted\ input] - Ct[IP]}$ (29, 74).

Luciferase reporter assay. The luciferase reporter assay and construct of h*DEL1* promoter/luciferase reporter plasmid (h*DEL1*-promoter-Luc) has been described in detail elsewhere (20). HMVECs were seeded into 96-well plates at a density of 1×10^4 cells per well and cotransfected with the h*DEL1*-promoter-Luc and pGL3 firefly luciferase reporter plasmid (Promega, Madison, Wisconsin, USA) as an internal transfection control using the 4D-Nucleofector V4XC for SF cell line (Lonza). HMVECs were treated with ethanol, ERM, JSM, or PC in the presence of IL-17 as described in the figure legends. Luciferase assay was performed using the Dual-Glo Luciferase Assay System and GloMax-Multi Detection System (Promega) according to the manufacturer's instructions.

Pulse oximetry. A portable mouse pulse oximeter (MouseOx PLUS, STARR Life Sciences, Oakmont, Pennsylvania, USA) was used to monitor SpO_2 and other physiological parameters (heart rate, breath rate, pulse distention) in free-roaming, nonanesthetized mice. The collars of experimental animals were trimmed of fur at least a day before the beginning of pulse oximetry monitoring. At indicated experimental time points, mice were anesthetized with 3% isoflurane in 100% oxygen for 2 minutes, and an extra-small MouseOx collar clip was placed on the animal's neck. Mice were allowed to recover from anesthesia (1–2 minutes) and pulse oximetry readings were recorded.

ELISA. Detection of human DEL-1 protein in the culture supernatants was performed by a sandwich ELISA as previously described (20) using serial dilutions of recombinant human DEL-1 (R&D Systems, Bio-Techne) for standard curve generation. TNF, IL-10, IL-6, and IL-17 levels in tissue lysates or serum were measured using a DuoSet ELISA Kit (R&D Systems, Bio-Techne) according to the manufacturer's instructions.

Determination of neutrophil numbers by flow cytometry. To obtain BALF, 1.0 mL PBS was instilled into mouse lungs and then slowly aspirated (3, 71). Single-cell suspensions from harvested gingival tissue were prepared according to a previously described method (75). The number of recruited neutrophils present in the BALF or gingival tissue was determined by flow cytometric analysis using Ly6G-allophycocyanin (1A8; BD Pharmingen, Franklin Lakes, New Jersey, USA) and CD11b-Alexa Fluor 488 (M1/7; BD Pharmingen) antibodies (14). Flow cytometric analysis of stained cells was performed on a NovoCyte flow cytometer (ACEA, San Diego, California, USA) and analyzed with NovoExpresss (ACEA).

Immunoblotting. Cell lysates were prepared using the RIPA Lysis Buffer System (Santa Cruz Biotechnology), and protein content concentrations were determined using the Bio-Rad Bradford protein assay. Proteins were separated by standard SDS with polyacrylamide gel electrophoresis on 10% acrylamide gels (Thermo Fisher Scientific) and transferred to polyvinylidene difluoride membranes (Bio-Rad, Hercules, California, USA) by electroblotting. The membranes were incubated in blocking buffer (StartingBlock; Thermo Fisher Scientific) followed by probing with primary antibodies and visualization with horseradish peroxidase–conjugated secondary antibody and chemiluminescence using MilliporeSigma ECL system. Images were captured using a FluorChem M imaging system (ProteinSimple, San Jose, California, USA). The sources of the various antibodies used are listed above under *Reagents*.

Quantitative real-time PCR. Total RNA was extracted from HMVECs and lung tissue using TRI Reagent (Molecular Research Center, Inc., Cincinnati, Ohio, USA) and quantified by spectrophotometry at 260 and 280 nm. The RNA was reverse-transcribed using SuperScript VILO Master Mix (Thermo Fisher Scientific), and qPCR with the cDNA was performed using the StepOnePlus real-time PCR system (Thermo Fisher Scientific) according to the manufacturer's protocol. Data were analyzed using the comparative CT (ΔΔCt) method. TaqMan probes, sense primers, and antisense primers for the expression of a housekeeping gene (*GAPDH*; Mm99999915_g1, *Gapdh*; Hs02786624_g1), as well as investigated genes *Edil3* (*Del1*) (*Del1*; Mm01291247_m1, *DEL1*; Hs00964112_m1), *Il6* (Mm00446190_m1), *Il1b* (Mm00434228_m1), *Tnf* (Mm00443258_m1), *Il10* (Mm01288386_m1), and *Il17a* (Mm00439618_m1), were purchased from Thermo Fisher Scientific.

Immunofluorescence and histological analysis. The lungs from mice subjected to LPS-induced lung inflammation were collected 48 hours or 5 days after LPS challenge. For standard histological and subsequent quantitative histomorphometric analyses, the lungs were fixed in 4% paraformaldehyde phosphate buffer solution (FUJIFILM Wako Pure Chemical Corporation) for 24 hours, then embedded in O.C.T. compound (Sakura Finetek Japan, Tokyo, Japan), followed by freezing of the samples in liquid nitrogen. Gingival biopsy specimens from mouse maxillae with intact surrounding tissue were fixed in 4% paraformaldehyde and

embedded in O.C.T. compound. Coronal sections were cut at 8 μm and mounted on glass slides. The sections were fixed in paraformaldehyde for 10 minutes and washed with a solution of PBS and 0.1% Tween-20 followed by PBS containing 0.1% Triton X-100, as well as PBS alone. Sections were stained using rabbit polyclonal antibody against DEL-1 (12480-1–AP; Proteintech) and rabbit polyclonal antibody against neutrophil elastase (ab68672; Abcam Japan, Tokyo, Japan), followed by Alexa Fluor 488–conjugated goat anti–rabbit IgG (A-11034; Thermo Fisher Scientific). The specificity of staining was confirmed by using appropriate isotype control (02-6100; Thermo Fisher Scientific) or nonimmune rabbit IgG (10500C: Thermo Fisher Scientific). Fluorescence images were captured using a confocal laser-scanning microscope (Carl Zeiss, Jena, Germany).

Immunofluorescence analysis of GHSR was performed using 70% confluent log phase HMVECs. The cells were fixed with 4% paraformaldehyde for 10 minutes, permeabilized with 0.1% Triton X-100 for 15 minutes, then blocked with 1% BSA for 1 hour at room temperature. The cells were labeled with GHSR polyclonal antibody (Thermo Fisher Scientific) at 5 μg/mL in 0.1% BSA, incubated overnight, and then labeled with goat anti–rabbit IgG (H+L) superclonal secondary antibody, Alexa Fluor 488 conjugate (Thermo Fisher Scientific), at a dilution of 1:2000 for 45 minutes at room temperature. Nuclei were stained with ProLong Diamond Antifade Mountant with DAPI (Thermo Fisher Scientific). F-actin was stained with rhodamine phalloidin (Thermo Fisher Scientific).

Statistics. Data were statistically evaluated by 1- or 2-way ANOVA. Tukey's multiple comparisons test was used for 1-way ANOVA. Holm-Šidák multiple comparisons test was used for 2-way ANOVA. Where appropriate (comparison of 2 groups only), unpaired 2-tailed *t* tests were conducted. The Kaplan-Meier survival curve was analyzed using the log-rank test equivalent to the Mantel-Haenszel test. All statistical analyses were performed using GraphPad Prism Software version 6.05 (GraphPad Software, Inc., La Jolla, California, USA). Values of $P < 0.05$ were considered significant.

Study approval. Genetic recombination–related mouse procedures were approved by the Genetic Recombination Experiment Safety Committee of Niigata University (SD00861). All animal experiments were approved by the Institutional Animal Care and Use Committee of Niigata University (SA00181).

Author contributions

T Maekawa contributed to conception, design, data acquisition, analysis, and interpretation and drafted and cowrote the manuscript; HT, TH, TI, DY, NH, and NT contributed to data acquisition, analysis, and interpretation; KT, T Maeda, MO, and HD contributed to data acquisition, analysis, and interpretation; AZ, VIA, TC, and YT contributed to conception and critically revised the manuscript. GH contributed to conception and design of the study, interpreted data, and cowrote the manuscript.

Acknowledgments

This work was supported by grants from JSPS KAKENHI (16H06272E, 17KK0165, 17K19747, 19H03828, 19K22706), the Senri Life Science Foundation, the Takeda Science Foundation, the Nakajima Foundation and young investigator research seed grant from JSP to TM, U.S. Public Health Service grants from the NIH (DE024716 to GH; DE028561 and DE026152 to GH and TC), a grant from the European Research Council (DEMETINL to TC), and grants from the Deutsche Forschungsgemeinschaft (SFB-TR 205 to TC and VIA and SFB1181 to TC).

Address correspondence to: Tomoki Maekawa, Center for Advanced Oral Science, Graduate School of Medical and Dental Sciences, 2-5274, Gakkocho-dori, Chuo-ku, Niigata-shi, 951-8514, Japan. Phone: 81.25.227.2828; Email: maekawa-t@dent.niigata-u.ac.jp.

1. Kanoh S, Rubin BK. Mechanisms of action and clinical application of macrolides as immunomodulatory medications. *Clin Microbiol Rev*. 2010;23(3):590–615.
2. Seemungal TA, Wilkinson TM, Hurst JR, Perera WR, Sapsford RJ, Wedzicha JA. Long-term erythromycin therapy is associated with decreased chronic obstructive pulmonary disease exacerbations. *Am J Respir Crit Care Med*. 2008;178(11):1139–1147.
3. Domon H, et al. Mechanism of macrolide-induced inhibition of pneumolysin release involves impairment of autolysin release in macrolide-resistant Streptococcus pneumoniae. *Antimicrob Agents Chemother*. 2018;62(11):e00161-18.
4. Southern KW, Barker PM, Solis-Moya A, Patel L. Macrolide antibiotics for cystic fibrosis. *Cochrane Database Syst Rev*. 2012;11:CD002203.
5. Albert RK, et al. Azithromycin for prevention of exacerbations of COPD. *N Engl J Med*. 2011;365(8):689–698.

6. Simoens S, Laekeman G, Decramer M. Preventing COPD exacerbations with macrolides: a review and budget impact analysis. *Respir Med*. 2013;107(5):637–648.
7. Walkey AJ, Wiener RS. Macrolide antibiotics and survival in patients with acute lung injury. *Chest*. 2012;141(5):1153–1159.
8. Rollins DR, Good JT, Martin RJ. The role of atypical infections and macrolide therapy in patients with asthma. *J Allergy Clin Immunol Pract*. 2014;2(5):511–517.
9. Zimmermann P, Ziesenitz VC, Curtis N, Ritz N. The immunomodulatory effects of macrolides-a systematic review of the underlying mechanisms. *Front Immunol*. 2018;9:302.
10. Plewig G, Schöpf E. Anti-inflammatory effects of antimicrobial agents: an in vivo study. *J Invest Dermatol*. 1975;65(6):532–536.
11. Kovaleva A, Remmelts HH, Rijkers GT, Hoepelman AI, Biesma DH, Oosterheert JJ. Immunomodulatory effects of macrolides during community-acquired pneumonia: a literature review. *J Antimicrob Chemother*. 2012;67(3):530–540.
12. Nagai K, Kimura O, Domon H, Maekawa T, Yonezawa D, Terao Y. Antimicrobial susceptibility of *Streptococcus pneumoniae*, *Haemophilus influenzae*, and *Moraxella catarrhalis* clinical isolates from children with acute otitis media in Japan from 2014 to 2017. *J Infect Chemother*. 2019;25(3):229–232.
13. Hajishengallis G, Chavakis T. DEL-1-regulated immune plasticity and inflammatory disorders. *Trends Mol Med*. 2019;25(5):444–459.
14. Kourtzelis I, et al. DEL-1 promotes macrophage efferocytosis and clearance of inflammation. *Nat Immunol*. 2019;20(1):40–49.
15. Choi EY, et al. Del-1, an endogenous leukocyte-endothelial adhesion inhibitor, limits inflammatory cell recruitment. *Science*. 2008;322(5904):1101–1104.
16. Mitroulis I, et al. Secreted protein Del-1 regulates myelopoiesis in the hematopoietic stem cell niche. *J Clin Invest*. 2017;127(10):3624–3639.
17. Eskan MA, et al. The leukocyte integrin antagonist Del-1 inhibits IL-17-mediated inflammatory bone loss. *Nat Immunol*. 2012;13(5):465–473.
18. Choi EY, et al. Developmental endothelial locus-1 is a homeostatic factor in the central nervous system limiting neuroinflammation and demyelination. *Mol Psychiatry*. 2015;20(7):880–888.
19. Mikacenic C, Hansen EE, Radella F, Gharib SA, Stapleton RD, Wurfel MM. Interleukin-17A is associated with alveolar inflammation and poor outcomes in acute respiratory distress syndrome. *Crit Care Med*. 2016;44(3):496–502.
20. Maekawa T, et al. Antagonistic effects of IL-17 and D-resolvins on endothelial Del-1 expression through a GSK-3β-C/EBPβ pathway. *Nat Commun*. 2015;6:8272.
21. Yan S, et al. Developmental endothelial locus-1 (Del-1) antagonizes Interleukin-17-mediated allergic asthma. *Immunol Cell Biol*. 2018;96(5):526–535.
22. Hashimoto M, Yamashita Y, Takemoto T. Electroporation of Cas9 protein/sgRNA into early pronuclear zygotes generates non-mosaic mutants in the mouse. *Dev Biol*. 2016;418(1):1–9.
23. Hashimoto M, Takemoto T. Electroporation enables the efficient mRNA delivery into the mouse zygotes and facilitates CRISPR/Cas9-based genome editing. *Sci Rep*. 2015;5:11315.
24. Kabir K, et al. Characterization of a murine model of endotoxin-induced acute lung injury. *Shock*. 2002;17(4):300–303.
25. Rittirsch D, et al. Acute lung injury induced by lipopolysaccharide is independent of complement activation. *J Immunol*. 2008;180(11):7664–7672.
26. Johnson KJ, Ward PA. Acute immunologic pulmonary alveolitis. *J Clin Invest*. 1974;54(2):349–357.
27. Hajishengallis G. Periodontitis: from microbial immune subversion to systemic inflammation. *Nat Rev Immunol*. 2015;15(1):30–44.
28. Dutzan N, et al. A dysbiotic microbiome triggers T_H17 cells to mediate oral mucosal immunopathology in mice and humans. *Sci Transl Med*. 2018;10(463):eaat0797.
29. Ziogas A, et al. DHEA inhibits leukocyte recruitment through regulation of the integrin antagonist DEL-1. *J Immunol*. 2020;204(5):1214–1224.
30. Uchimura T, et al. Erythromycin acts through the ghrelin receptor to attenuate inflammatory responses in chondrocytes and maintain joint integrity. *Biochem Pharmacol*. 2019;165:79–90.
31. Kojima M, Hosoda H, Matsuo H, Kangawa K. Ghrelin: discovery of the natural endogenous ligand for the growth hormone secretagogue receptor. *Trends Endocrinol Metab*. 2001;12(3):118–122.
32. Kojima M, Hosoda H, Date Y, Nakazato M, Matsuo H, Kangawa K. Ghrelin is a growth-hormone-releasing acylated peptide from stomach. *Nature*. 1999;402(6762):656–660.
33. Jeon SG, et al. Ghrelin in Alzheimer's disease: pathologic roles and therapeutic implications. *Ageing Res Rev*. 2019;55:100945.
34. Park YJ, et al. Ghrelin enhances the proliferating effect of thyroid stimulating hormone in FRTL-5 thyroid cells. *Mol Cell Endocrinol*. 2008;285(1-2):19–25.
35. Chung H, Li E, Kim Y, Kim S, Park S. Multiple signaling pathways mediate ghrelin-induced proliferation of hippocampal neural stem cells. *J Endocrinol*. 2013;218(1):49–59.
36. Kim C, Kim S, Park S. Neurogenic effects of ghrelin on the hippocampus. *Int J Mol Sci*. 2017;18(3):E588.
37. Lebel M. Pharmacokinetic properties of clarithromycin: a comparison with erythromycin and azithromycin. *Can J Infect Dis*. 1993;4(3):148–152.
38. Zuckerman JM, Qamar F, Bono BR. Macrolides, ketolides, and glycylcyclines: azithromycin, clarithromycin, telithromycin, tigecycline. *Infect Dis Clin North Am*. 2009;23(4):997–1026.
39. Giamarellos-Bourboulis EJ, et al. Effect of clarithromycin in patients with suspected Gram-negative sepsis: results of a randomized controlled trial. *J Antimicrob Chemother*. 2014;69(4):1111–1118.
40. Majima Y. Clinical implications of the immunomodulatory effects of macrolides on sinusitis. *Am J Med*. 2004;117(suppl 9A):20S–25S.
41. Xu Y, et al. Ghrelin inhibits the differentiation of T helper 17 cells through mTOR/STAT3 signaling pathway. *PLoS One*. 2015;10(2):e0117081.
42. Orlova EG, Shirshev SV. Role of leptin and ghrelin in induction of differentiation of IL-17-producing and T-regulatory cells. *Bull Exp Biol Med*. 2014;156(6):819–822.
43. Reis BS, et al. Leptin receptor signaling in T cells is required for Th17 differentiation. *J Immunol*. 2015;194(11):5253–5260.
44. Kassebaum NJ, Bernabé E, Dahiya M, Bhandari B, Murray CJ, Marcenes W. Global burden of severe periodontitis in 1990-

2010: a systematic review and meta-regression. *J Dent Res*. 2014;93(11):1045–1053.
45. Chapple IL. Time to take periodontitis seriously. *BMJ*. 2014;348:g2645.
46. Peres MA, et al. Oral diseases: a global public health challenge. *Lancet*. 2019;394(10194):249–260.
47. Shin J, et al. DEL-1 restrains osteoclastogenesis and inhibits inflammatory bone loss in nonhuman primates. *Sci Transl Med*. 2015;7(307):307ra155.
48. Yuh DY, et al. The secreted protein DEL-1 activates a β3 integrin-FAK-ERK1/2-RUNX2 pathway and promotes osteogenic differentiation and bone regeneration. *J Biol Chem*. 2020;295(21):7261–7273.
49. Castillo RL, Carrasco Loza R, Romero-Dapueto C. Pathophysiological approaches of acute respiratory distress syndrome: novel bases for study of lung injury. *Open Respir Med J*. 2015;9:83–91.
50. Pinheiro NM, et al. Pulmonary inflammation is regulated by the levels of the vesicular acetylcholine transporter. *PLoS One*. 2015;10(3):e0120441.
51. Namkoong H, et al. Clarithromycin expands CD11b+Gr-1+ cells via the STAT3/Bv8 axis to ameliorate lethal endotoxic shock and post-influenza bacterial pneumonia. *PLoS Pathog*. 2018;14(4):e1006955.
52. Ito T, Ito N, Hashizume H, Takigawa M. Roxithromycin inhibits chemokine-induced chemotaxis of Th1 and Th2 cells but regulatory T cells. *J Dermatol Sci*. 2009;54(3):185–191.
53. Sato Y, Kaneko K, Inoue M. Macrolide antibiotics promote the LPS-induced upregulation of prostaglandin E receptor EP2 and thus attenuate macrolide suppression of IL-6 production. *Prostaglandins Leukot Essent Fatty Acids*. 2007;76(3):181–188.
54. Davidson R, Péloquin L. Anti-inflammatory effects of the macrolides. *J Otolaryngol*. 2002;31(suppl 1):S38–S40.
55. Wales D, Woodhead M. The anti-inflammatory effects of macrolides. *Thorax*. 1999;54(suppl 2):S58–S62.
56. Tamaoki J, Kadota J, Takizawa H. Clinical implications of the immunomodulatory effects of macrolides. *Am J Med*. 2004;117(suppl 9A):5S–11S.
57. He ZY, et al. Effect of 6 months of erythromycin treatment on inflammatory cells in induced sputum and exacerbations in chronic obstructive pulmonary disease. *Respiration*. 2010;80(6):445–452.
58. Banerjee D, Honeybourne D, Khair OA. The effect of oral clarithromycin on bronchial airway inflammation in moderate-to-severe stable COPD: a randomized controlled trial. *Treat Respir Med*. 2004;3(1):59–65.
59. Righetti RF, et al. Protective effects of anti-IL17 on acute lung injury induced by LPS in mice. *Front Pharmacol*. 2018;9:1021.
60. Sanger GJ, Furness JB. Ghrelin and motilin receptors as drug targets for gastrointestinal disorders. *Nat Rev Gastroenterol Hepatol*. 2016;13(1):38–48.
61. Tomasetto C, et al. Identification and characterization of a novel gastric peptide hormone: the motilin-related peptide. *Gastroenterology*. 2000;119(2):395–405.
62. Westaway SM, Sanger GJ. The identification of and rationale for drugs which act at the motilin receptor. *Prog Med Chem*. 2009;48:31–80.
63. Matsuura B, Dong M, Naik S, Miller LJ, Onji M. Differential contributions of motilin receptor extracellular domains for peptide and non-peptidyl agonist binding and activity. *J Biol Chem*. 2006;281(18):12390–12396.
64. Murray CD, et al. Ghrelin enhances gastric emptying in diabetic gastroparesis: a double blind, placebo controlled, crossover study. *Gut*. 2005;54(12):1693–1698.
65. Sun Y, Wang P, Zheng H, Smith RG. Ghrelin stimulation of growth hormone release and appetite is mediated through the growth hormone secretagogue receptor. *Proc Natl Acad Sci U S A*. 2004;101(13):4679–4684.
66. Smith RG, Jiang H, Sun Y. Developments in ghrelin biology and potential clinical relevance. *Trends Endocrinol Metab*. 2005;16(9):436–442.
67. Beiras-Fernandez A, et al. Altered myocardial expression of ghrelin and its receptor (GHSR-1a) in patients with severe heart failure. *Peptides*. 2010;31(12):2222–2228.
68. Folwaczny M, Karnesi E, Berger T, Paschos E. Clinical association between chronic periodontitis and the leukocyte extravasation inhibitors developmental endothelial locus-1 and pentraxin-3. *Eur J Oral Sci*. 2017;125(4):258–264.
69. Colburn WA, Di Santo AR, Gibaldi M. Pharmacokinetics of erythromycin on repetitive dosing. *J Clin Pharmacol*. 1977;17(10 Pt 1):592–600.
70. Hajishengallis G, Wang M, Bagby GJ, Nelson S. Importance of TLR2 in early innate immune response to acute pulmonary infection with Porphyromonas gingivalis in mice. *J Immunol*. 2008;181(6):4141–4149.
71. Domon H, et al. Neutrophil elastase subverts the immune response by cleaving Toll-like receptors and cytokines in pneumococcal pneumonia. *Front Immunol*. 2018;9:732.
72. Moriyama C, et al. Aging enhances susceptibility to cigarette smoke-induced inflammation through bronchiolar chemokines. *Am J Respir Cell Mol Biol*. 2010;42(3):304–311.
73. Maekawa T, et al. Differential expression and roles of secreted frizzled-related protein 5 and the wingless homolog Wnt5a in periodontitis. *J Dent Res*. 2017;96(5):571–577.
74. Lin X, Tirichine L, Bowler C. Protocol: chromatin immunoprecipitation (ChIP) methodology to investigate histone modifications in two model diatom species. *Plant Methods*. 2012;8(1):48.
75. Dutzan N, Abusleme L, Konkel JE, Moutsopoulos NM. Isolation, characterization and functional examination of the gingival immune cell network. *J Vis Exp*. 2016;(108):53736.